Technical Note

# Robust and low-cost ELISA based on IgG-Fc tagged recombinant proteins to screen for anti-SARS-CoV-2 antibodies

Etienne Frumence [a,b,*], Grégorie Lebeau [a,b], Wildriss Viranaicken [c], Anthony Dobi [a,b], Damien Vagner [b,c], Mahary Lalarizo Rakoto [a,b,d], Anne-Laure Sandenon Seteyen [a,b], Claude Giry [e], Axelle Septembre-Malaterre [a,b], Loïc Raffray [c,f], Philippe Gasque [a,b]

[a] Unité de recherche en Pharmaco-Immunologie (UR-EPI), Université et CHU de La Réunion, Saint-Denis 97400, France
[b] Laboratoire d'immunologie Clinique et expérimentale de la ZOI (LICE-OI), Pôle de Biologie, CHU de La Réunion, Saint-Denis 97400, France
[c] UMR PIMIT 'Processus Infectieux en Milieu Insulaire Tropical' CNRS 9192, INSERM1187, IRD 249, Université de La Réunion, Saint-Denis 97400, France
[d] Faculté de Médecine, Campus universitaire Ambohitsaina, BP375, Université d'Antananarivo, Madagascar
[e] CNR associé arbovirus, Laboratoire de Microbiologie, Pôle de Biologie, CHU de La Réunion, Saint-Denis 97440, France
[f] Service de Médecine Interne, Centre Hospitalier Universitaire La Réunion Site Félix Guyon, CS11021, 97400 Saint Denis de La Réunion, France

## ARTICLE INFO

## ABSTRACT

The development of new diagnostic assays become a priority for managing COVID-19. To this aim, we presented here an in-house ELISA based on the production of two major recombinant and high-quality antigens from SARS-CoV-2. Full-length N and S-RBD fragment proteins fused to mouse IgG2a-Fc were produced in the CHO cell line. Secreted recombinant proteins were easily purified with standard Protein A chromatography and were used in an in-house ELISA to detect anti-N and anti-RBD IgGs in the plasma of COVID-19 RTPCR-positive patients. High reactivity against recombinant antigens was readily detected in all positive plasma samples, whereas no recognition was observed with control healthy subject's plasmas. Remarkably, unpurified recombinant N protein obtained from cell culture supernatant was also suitable for the monitoring by ELISA of IgG levels in positive patients. This work provides an early prospection for low price but high-quality serological kit development.

## 1. Introduction

The SARS-CoV-2 (severe acute respiratory syndrome coronavirus-2) responsible for COVID-19 (Coronavirus infectious disease 2019) emerged as a novel human pathogen in December 2019, and still threatens global public health to date (Lebeau et al., 2020; Wang et al., 2021; Zhou et al., 2020). This virus is a positive-sense single stranded RNA virus that encodes four structural proteins: the N (Nucleocapsid), M (membrane), E (Envelope), and S (Spike) proteins. Among them, the N protein is abundantly expressed during infection and is highly immunogenic (Burbelo et al., 2020). Whereas S protein contains a receptor-binding domain (RBD) that specifically recognizes angiotensin-converting enzyme 2 (ACE2) as its receptor on the host cells, making it the main target for neutralizing antibodies (Rogers et al., 2020; Walls et al., 2020).

Studies on SARS-CoV and SARS-CoV-2 infections have suggested that early antibody response was directed against the N and S proteins (Burbelo et al., 2020). Of note, seroconversion appears generally 13 days after symptoms onset during COVID-19, with IgG and IgM production occurring almost simultaneously (Burbelo et al., 2020; Long et al., 2020).

To monitor ongoing infection in a patient, SARS-CoV-2 genome can be detected by RT-PCR in nasopharyngeal sample. However, serological assays are critically needed to obtain information about individual past-exposure, to conduct epidemiological studies, to confirm ambiguous RT-PCR results and to understand the immune response to this virus. The availability of specific, sensitive and low-cost serological tests is therefore highly needed to help control the spread of this disease.

Herein, we provide a robust and low-cost method for small laboratories around the world, even with modest experience in protein expression and purification, to produce high quality antigens suitable for serology and biochemical assays. The in-house ELISA described here is based on recombinant full-length N and S-RBD fragment proteins fused to mouse IgG2a-Fc produced in a mammalian cell line. The final

proteins produced in stable cell lines were used as antigens and were readily usable without purification steps in ELISA.

## 2. Materials and methods

### 2.1. Cells and reagents

Chinese hamster ovary (CHO) cells and epithelial Vero cells were cultured at 37 °C under 5% $CO_2$ atmosphere in Ham's F12 medium and MEM Eagle medium respectively, supplemented with 10% heat-inactivated fetal bovine serum, 2 mM L-Glutamine, 1 mM sodium pyruvate, 100 U/mL of penicillin, 0.1 mg/mL of streptomycin and 0.5 μg/mL of amphotericin B (PAN Biotech, Aidenbach, Germany). The horseradish peroxidase conjugated goat anti-mouse IgG (#172-1011) and mouse anti-human IgG (#9040-05) were purchased from Biorad, Hercule, CA, USA and Southern Biotech, Birmingham, AL, USA, respectively.

### 2.2. Stable transfection of CHO cells with vector plasmid expressing SARS-CoV-2 viral antigens

The production of recombinant SARS-CoV-2 proteins was based on mammalian codon-optimized sequences encoding the full-length SARS-CoV-2 Nucleocapsid (NCI Gene ID: **43560237**) or the fragment containing 223 residues (aa 319-541) of the Spike protein Receptor Binding Domain (GenBank accession number: **QHR63250.1**) followed by the mouse IgG2a-Fc Tag sequence (optimized residues 295–993; GenBank accession number: **V00798.1**). Upstream of these sequences, an optimized secretion sequence (Barash et al., 2002) and a Kozak consensus sequence were added. To ensure a high expression level an EF-1α promoter sequence was added (Kim et al., 1990). The cDNA synthesis and molecular cloning in pcDNA3.1(+) Hygro plasmid were done by GeneCust (Luxembourg) at the BamHI and *Xba*I sites. Recombinant plasmids pcDNA3.1/N$^{IgG2a-Fc}$ and pcDNA3.1/S-RBD$^{IgG2a-Fc}$ were generated. CHO cells were transfected with pcDNA3.1/N$^{IgG2a-Fc}$ and pcDNA3.1/S-RBD$^{IgG2a-Fc}$ plasmids using Lipofectamine 3000 (#L3000-008, Invitrogen, Carlsbad, CA, USA) according to the manufacturer's instructions to generate CHO/rN and CHO/rRBD. Cells were then selected in culture medium supplemented with 400 μg/mL hygromycin B (#10687010, Invitrogen, Carlsbad, CA, USA) and cloned by limiting dilution.

### 2.3. Production and purification of recombinant SARS-CoV-2 proteins

To purify secreted rN and rRBD, stable transfected CHO cell monolayers were cultured for 4 days with Panserin 401 medium (#P04-710401, PAN Biotech, Aidenbach, Germany) optimized for serum-free cell cultivation to reduce bovine IgG contamination. The harvested culture medium (150 mL) was filtered and then concentrated using Amicon Ultra15 centrifugal device with a 10 kDa cut-off (Millipore, Burlington, MA, USA). The samples were loaded on a 1 mL HiTrap Protein A HP prepacked column (#17-0402-03, GE healthcare, Chicago, IL, USA), according to the manufacturer's protocol. After a washing step with 10 mL of 20 mM sodium phosphate pH 7.5, bound Fc-IgG2a-tagged proteins were eluted from affinity column with 0.1 M citric acid pH 4.5. The eluted fractions were neutralized with 1 M Tris-HCl, pH 9.0. All fractions were verified for the presence of recombinant Fc-IgG2a-tagged proteins by Dot-Blot assay. According to Dot-Blot assay, the elution samples containing purified recombinant proteins were concentrated using Amicon Ultra15 centrifugal device with a 10 kDa cut-off and stored at −80 °C.

Protein quantification of the purified recombinant protein was performed using Bradford assay (Sigma-Aldrich, St. Louis, MS, USA). Biochemical evaluation of rN and rRBD was conducted by SDS-PAGE with Coomassie-blue staining and Western Blot, described hereafter.

### 2.4. Immunoblot assay

Western Blot assay was essentially performed as previously described (Frumence et al., 2019). Briefly, cells were lyzed with Triton lysis buffer, supplemented with protease inhibitor cocktail and concentration of proteins in the cell lysates was quantified using Bradford protein assay. Proteins were loaded on NuPAGE 4 to 12% bis-Tris protein gel (Invitrogen, Carlsbad, CA, USA) and transferred to a 0.45 μm Amersham protan nitrocellulose membrane (GE healthcare, Chicago, IL, USA). After blocking, the membrane was incubated with appropriate dilutions of human plasma (dilution 1:1000). Mouse anti-Human IgG HRP-conjugate was used as secondary antibody (dilution 1:5000), while goat anti-mouse IgG HRP-conjugate was used to detect directly the IgG2a-Fc tag (dilution 1:5000). Revelation was done using Amersham ECL prime Western Blotting Detection Reagent (GE healthcare, Chicago, IL, USA) and acquired with a Fusion Fx Spectra imager (Vilber, Marne-la-Vallée, France).

For Dot-Blot assays, 100 μL of elution samples were directly loaded on a nitrocellulose membrane using a Milliblot apparatus (Millipore, Burlington, MA, USA) and then probed with antibodies as aforementioned.

### 2.5. Indirect ELISA

Indirect in-house ELISA was used to measure the production of anti-N and anti S-RBD IgGs in patient's plasmas. Nunc MaxiSorp flat-bottom 96-well plates (Thermo Fisher Scientific, Waltham, MA, USA) were coated with 15 ng of rN or rRBD per well overnight at 4 °C, using either purified proteins or cell culture supernatant (1,10 dilution in PBS). Afterwards, wells were washed with PBS 0.1% Tween 20 and blocked for 30 min in blocking buffer (PBS with 0.1% Tween 20 and 5% Milk) at 25 °C. Coated plates were incubated with patient's plasmas at 1:400 dilution in blocking buffer. After washing, wells were incubated with a 1:10,000 dilution of horseradish peroxidase conjugated-mouse anti-human IgG antibodies for 1 h. Wells were washed with PBS-Tween 20 0.1% three times and the horseradish peroxidase activity was revealed using 3,3′,5,5′-tetramethylbenzidine (TMB solution, Invitrogen, Carlsbad, CA, USA) as HRP substrate and stopped with HCl 0.1 M. Absorbance was read at 450 nm, with a reference at 630 nm, using a 800TS microplate reader (Biotek Winooski, VT, USA).

The commercial Human COVID-19 IgG antibody ELISA kit (#MBS3809906, MyBiosource, San Diego, CA, USA) was used to detect anti-N IgG, according to the manufacturer's instructions. Plasma samples were used at a 1:400 dilution.

### 2.6. Ethical statement

Patients with RT-PCR-confirmed COVID-19 consented for the testing at the time of entry at the hospital (CHU de la Réunion). Samples were deposited at the local BioResource Centre (CRB, certified by EuroQuality System, NF 996–900) and declared in the local bio-collection of infectious diseases. A total of 16 positive patient's plasmas collected at least 13 days after symptom onset were selected in this study and were confirmed by ELISA (Fig. S1).

For negative controls, 8 plasma samples from healthy donors from the University and CHU of La Réunion were used under informed consent.

### 2.7. Data curation

Data processing and figure drawing were performed by Prism software version 7.01 (GraphPad, San Diego, CA, USA). The cut-off level between positive and negative plasma was taken as the mean absorbance of the negative controls plus three times the standard deviation.

# 3. Results and discussion

## 3.1. Expression and purification of recombinant SARS-CoV-2 N and RBD proteins in CHO cells

### 3.1.1. Production

To produce SARS-CoV-2 antigens for the development of serology assays, we selected the CHO cell line that emerged as the gold standard for rapid and efficient production of recombinant proteins given their very robust growth (Wurm, 2004). In order to produce recombinant N and RBD proteins of SARS-CoV-2, modifications that optimize the expression of viral gene in mammalian cells were done on original sequences. The N and RBD sequences were inserted into pcDNA3.1(+) Hygro. In this construct, SARS-CoV-2 N or RBD sequence was preceded by an artificial optimized secretion sequence (Barash et al., 2002), and ended with a mouse IgG2a-Fc tag sequence (Fig. 1A). The IgG-Fc fusion tag can be easily purified using standard protein A or G affinity chromatography and is readily detected by immunodetection using anti-mouse IgG antibodies. Also, it has been widely acknowledged that the addition of IgG-Fc fragment could increase protein stability, solubility, immunogenicity and expression yield (Czajkowsky et al., 2012).

CHO cells were transfected with pcDNA3.1/N$^{IgG2a-Fc}$ or pcDNA3.1/S-RBD$^{IgG2a-Fc}$, selected on growth medium supplemented with Hygromycin B and cloned by limiting dilution to establish stable cell lines CHO/rN and CHO/rRBD.

Of note, the expected molecular weight of SARS-CoV-2 N protein was 48.7 kDa and S-RBD fragment was 28 kDa. Moreover, the mouse IgG2a-Fc has a calculated molecular weight of 26.26 kDa and is known to migrate at around 35 kDa under reducing condition as a result of glycosylation and around 70 kDa under non-reducing condition in SDS-PAGE most-likely due to dimerization by disulfide bridges (Zhao et al., 2018).

Lysates and supernatants of the different transfected cells were analyzed in SDS-PAGE using anti-mouse IgG mAb (Fig. 1B). The presence of recombinant N (rN) and RBD (rRBD) were clearly detected in transfected CHO cell lysates. Recombinant N and RBD were also secreted in the supernatant. Under non-reducing conditions, bands detected for recombinant IgG2a-Fc tagged N at approximately 200 kDa were higher than the theoretical molecular weight (~170 kDa) probably due to phosphorylation of the Nucleocapsid (Surjit et al., 2005). The recombinant RBD migrated at approximately 130 kDa, which was consistent with the expected sizes of fusion protein homodimers (Fig. 1B).

In supernatant from CHO/rN, several bands were detected for the rN suggesting proteolysis of this protein. It has been already observed that cleavage of Nucleocapsid from SARS-CoV could occur in a cell-specific manner, leading to several smaller fragments in infected cells or during production of recombinant proteins (Diemer et al., 2008; Mark et al., 2008).

## 3.2. Purification

Then, IgG2a-Fc tagged rN and rRBD were purified from supernatant of CHO/rN and CHO/rRBD by standard protein A based affinity chromatography. Dot Blot assay using anti-mouse IgG mAb confirmed that the elution samples contained the recombinant Fc-IgG2a-tagged proteins (Fig. 2A and E). This purification step allowed us to recover 115 and 75 μg of rN and rRBD respectively from 150 mL of culture supernatant, with a purity of at least 90% as determined by SDS-PAGE with Coomassie Blue staining (Fig. 2B and F). Monomer of rN and rRBD were obtained after addition of 5% β-Mercaptoethanol and heat-denaturation. In reducing conditions, the apparent molecular weights of recombinant N and RBD were around 100 kDa and 60–65 kDa respectively which were consistent with the expected molecular weight of fusion protein monomers (Fig. 2B and F).

Subsequently, we assessed protein antigenicity with a Western Blot analysis using plasmas from positive and negative COVID-19 patients (Fig. 2C, D, G and H). We observed that non-reduced dimer of rN and rRBD were detected with the pool of positive plasmas while no bands were observed with the pool of control plasmas. In reducing conditions, only rN was detected with positive plasmas (Fig. 2G).

These results confirmed that the transfection of CHO cells with pcDNA3.1/N$^{IgG2a-Fc}$ or pcDNA3.1/S-RBD$^{IgG2a-Fc}$ vectors leads to efficient secretion of antigenic recombinant N and RBD that could be easily purified with standard Protein A chromatography.

### 3.2.1. In-house ELISA to test for antigenic reactivity of human plasma samples on rN and rRBD antigens

To evaluate the sensitivity of an ELISA based on rN and rRBD proteins, a dose-response curve was performed using either pooled positive or negative plasmas (Fig. 3A and C). Recombinant protein-based ELISA revealed positive plasma ability to react against rN and rRBD. For rN, the detection limit was about 0.02 μg/mL (2 ng per well of 96-well plate) whereas the plateau was reached at 0.8 μg/mL. For rRBD, detection limit was about 0.04 μg/mL (4 ng per well of 96-well plate) whereas the plateau was reached at around 1 μg/mL. A concentration of 0.15 μg/mL (15 ng per well of 96-well plate) was used for following recombinant protein-based ELISA. Indeed, this concentration permitted no recognition with control plasma and an acceptable signal-to-noise ratio.

We then examined the antigenic reactivity of 16 individually confirmed positive patient's plasmas collected at least 13 days after symptom onset against recombinant SARS-CoV-2 proteins by indirect ELISA. Antigenic reactivity of these positive plasmas was confirmed with a commercial anti-N ELISA (Fig. S1). Using purified rN or rRBD-based in-house ELISA, reactivity was readily detected in all positive plasma samples, whereas no recognition was observed with 8 individual negative control plasmas (Fig. 3B and D). No background noise was observed in our recombinant protein-based ELISA using purified proteins.
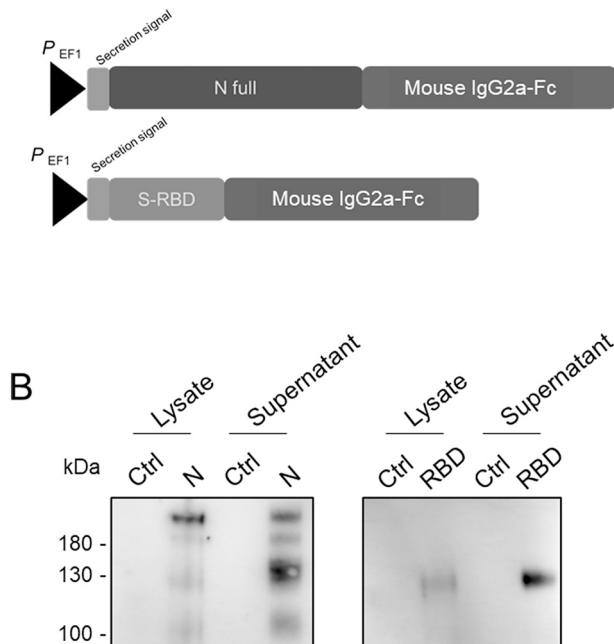


**Fig. 1.** Schematic representation of the cloning strategy (A) and characterization of recombinant N and RBD produced in CHO cells (B). In (A), the mammalian codon-optimized sequence encoding the full-length SARS-CoV-2 Nucleocapsid (N full) or the Spike Receptor Binding Domain (RBD), preceded by an artificial secretory signal sequence, was fused to the mouse IgG2a-Fc domain and cloned into the plasmid vector pcDNA3.1. In (B), the expression of recombinant SARS-CoV-2 N and RBD in CHO cells stably transfected with pcDNA3.1/N$^{IgG2a-Fc}$ or pcDNA3.1/S-RBD$^{IgG2a-Fc}$ plasmid vector was evaluated by Western Blot analysis in cell lysate or supernatant from transfected CHO/rN and CHO/rRBD and mock transfected control CHO (Ctrl) cells.
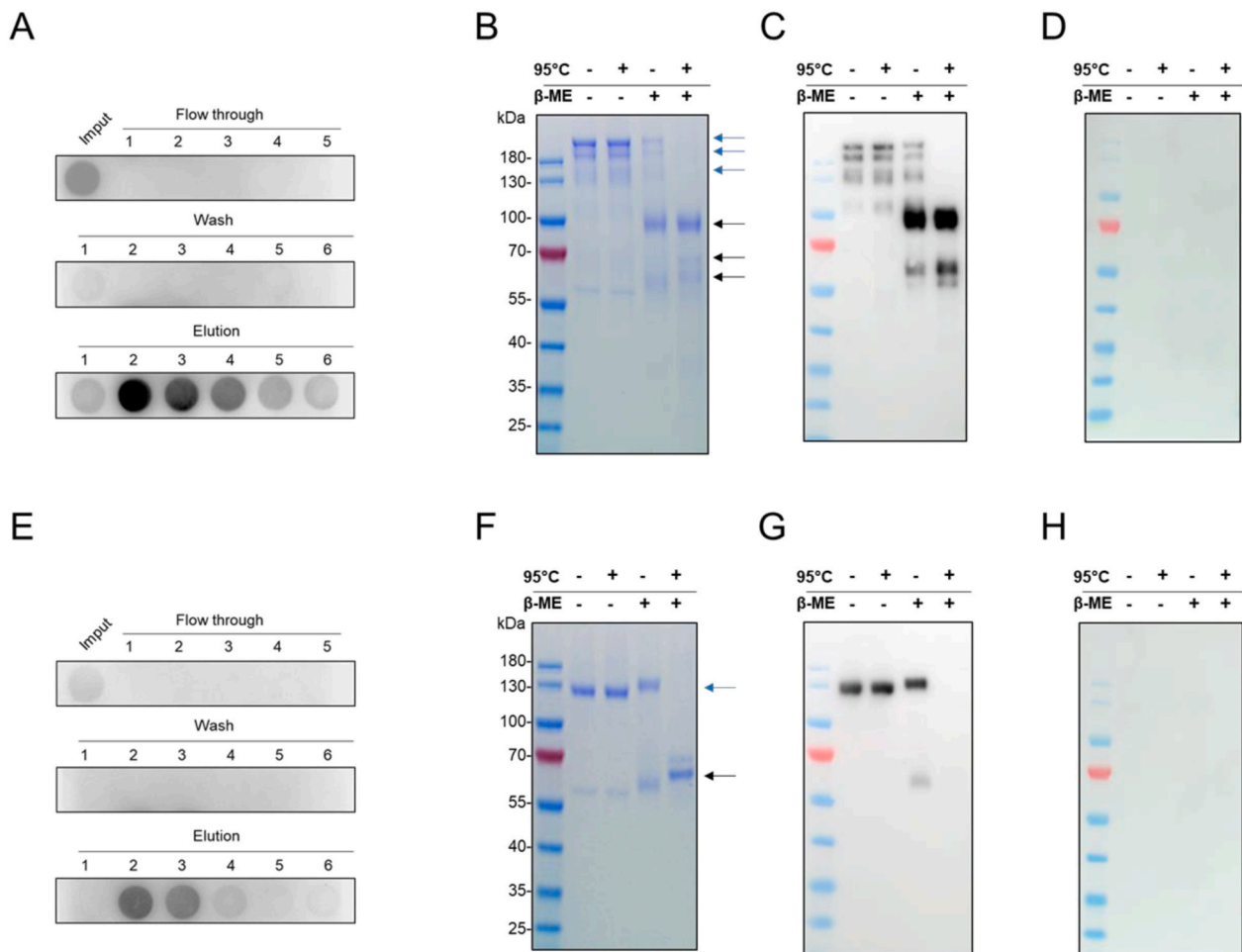
**Fig. 2.** Purification and biochemical evaluation of the recombinant N (A–D) and RBD (E–H) proteins. Recombinant proteins from concentrated supernatant were purified by protein A affinity chromatography. In (A and E), all fractions were verified for the presence of recombinant Fc-IgG2a-tagged proteins by Dot-Blot assay using goat anti-mouse IgG mAb. In (B and F), rN and rRBD purity were evaluated by SDS-PAGE followed by Coomassie blue staining. Samples were either heat-denatured (95 °C) or reduced with 5% β-mercaptoethanol (β-ME). The band corresponding to fc-tagged dimers (blue arrow) or monomers (black arrow) are indicated to the right of the gel. In (C and G), samples of purified rN and rRBD were analyzed by immunoblotting with a pool of positive plasma samples. In (D and H), samples of purified rN and rRBD were analyzed by immunoblotting with a pool of negative plasma samples. (For interpretation of the references to colour in this figure legend, the reader is referred to the web version of this article.)

These results demonstrate that purified rN and rRBD were relevant antigens that could be used in an in-house ELISA to detect anti-N and anti-RBD IgGs.

Serological studies of SARS-CoV patients showed that specific antibodies against the N protein appeared in the early stage of infection between day 8 to 14 after initial symptoms with a higher sensitivity than spike protein-directed antibodies (Burbelo et al., 2020; Leung et al., 2004). Using Western Blot analysis, we observed that pooled positive plasmas detected a major band at 50 kDa that likely corresponded to the Nucleocapsid in SARS-CoV-2 infected Vero cells lysate (Fig. S2). Using our rN (mixed with positive plasma samples), we could deplete this band, confirming that the early antibody response of COVID-19 patients targets the viral Nucleocapsid, as observed also by others authors (Burbelo et al., 2020; Leung et al., 2004; Long et al., 2020). Moreover, this result demonstrated once again that our rN protein was an appropriate antigen that reacts with anti-N IgGs.

Intriguingly, we observed that CHO/rN cells produced more recombinant proteins than CHO/rRBD cells and determined by indirect ELISA that supernatant from CHO/rN contains around 0.8 μg/mL of rN (data not shown). We therefore cultivated CHO/rN with serum-free Panserin medium and directly used the cell culture supernatant for ELISA at 0.15 μg/mL of rN. As shown in Fig. 4, unpurified rN antigen in supernatant was suitable to detect IgG from positive plasma samples. Antigenic reactivity of positive patient's plasma was detected in all 16 samples, whereas no recognition was observed with 8 individual control patient's plasma (Fig. 4). Taken together these results demonstrated that even unpurified recombinant N was a readily useful antigen to monitor specific IgG levels.

The estimated cost of our in-house ELISA based on unpurified recombinant N protein derived from cell culture supernatant was less than US$0.10 per test. This work provides an early prospection for low price but high-quality diagnostic kit development.

Some limitations in our assay development exist and need to be addressed in future studies. The cohort sample size was limited, so proper optimization and validation under large-scale conditions with more COVID-19 patient samples are required. In addition, cross reactivity of this assay in patients with other coronaviruses infection must be evaluated.

## 4. Concluding remarks

The development of new serological assays is becoming a high priority for managing SARS-CoV-2 epidemic. To this aim, we presented herein the production of two major recombinant and high-quality
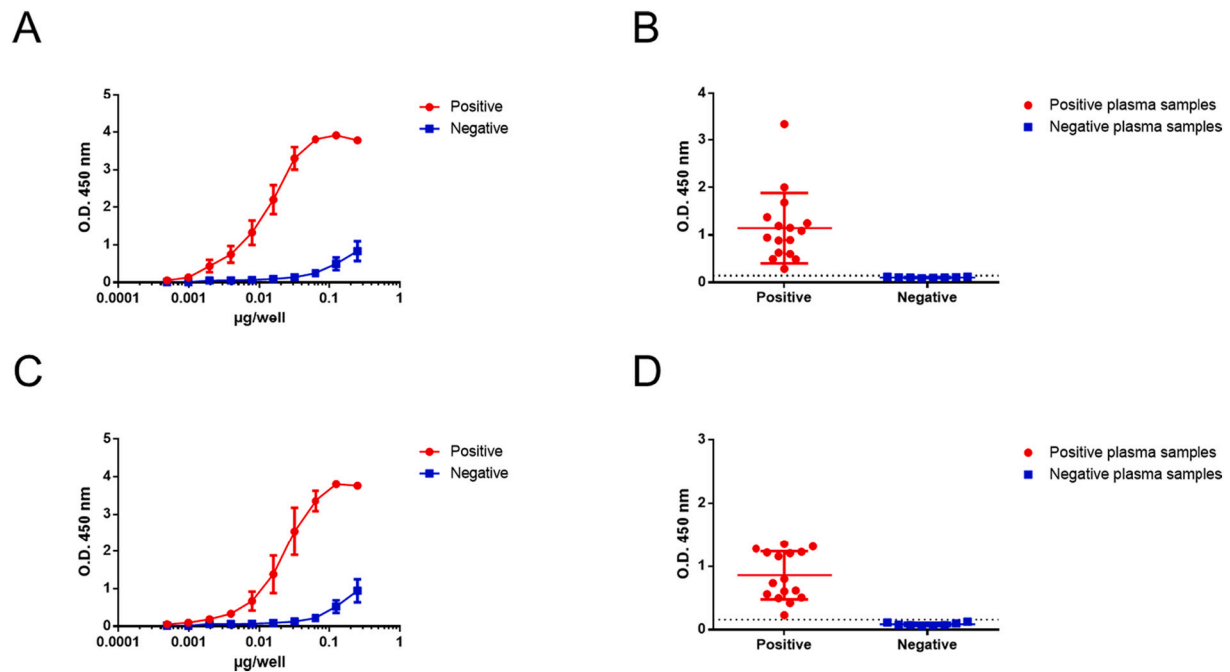
**Fig. 3.** Reactivity of human plasma samples on rN (A and B) and rRBD (C and D) antigens by indirect ELISA assay. In (A and C), plates were coated with increasing concentrations of rN or rRBD and incubated with a pooled of 5 positive or negative plasma samples at dilution 1:400. In (B or D), recombinant proteins were coated at 15 ng/well and incubated with 16 positive or 8 negative individual plasma samples at dilution 1:400. Horizontal dashed lines correspond to the cutoff value of the assay (0.137 for B and 0.159 for D).
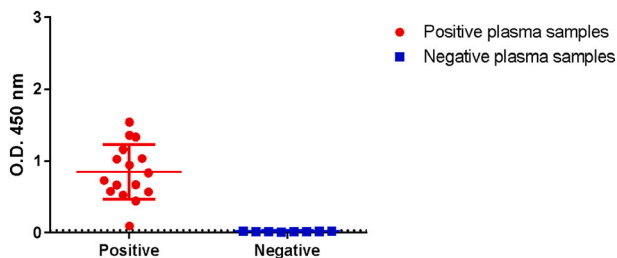


**Fig. 4.** Reactivity of human plasma samples on unpurified N antigen in supernatant by indirect ELISA assay. Plates were coated with approximately 15 ng/well of unpurified N antigen in cell culture Panserin supernatant and incubated with 16 positive or 8 negative individual plasma samples at dilution 1:400. The horizontal dashed line corresponds to the cutoff value of the assay (0.04).

antigens of SARS-CoV-2 virus that allow the establishment of serological assays. These reagents could also be used for biochemical assays, as well as structural biology or vaccine strategy studies. The high quality of these proteins, especially rN, allowed us to use of unpurified cell culture supernatant directly in an in-house ELISA. We greatly hope that the strategy highlighted in this communication will help others in the development of in-house diagnostic kit, to overcome the shortage and soaring price of commercial serological assay.

*Conflicts of interest*

The authors declare no conflict of interest.

## Appendix A. Supplementary data

Supplementary data to this article can be found online at https://doi.org/10.1016/j.jim.2021.113082.

## References

Barash, S., Wang, W., Shi, Y., 2002. Human secretory signal peptide description by hidden Markov model and generation of a strong artificial signal peptide for secreted protein expression. Biochem. Biophys. Res. Commun. 294, 835–842. https://doi.org/10.1016/S0006-291X(02)00566-1.

Burbelo, P.D., Riedo, F.X., Morishima, C., Rawlings, S., Smith, D., Das, S., Strich, J.R., Chertow, D.S., Davey, R.T., Cohen, J.I., 2020. Sensitivity in detection of antibodies to nucleocapsid and spike proteins of severe acute respiratory syndrome coronavirus 2 in patients with coronavirus disease 2019. J. Infect. Dis. 222, 206–213. https://doi.org/10.1093/infdis/jiaa273.

Czajkowsky, D.M., Hu, J., Shao, Z., Pleass, R.J., 2012. Fc-fusion proteins: new developments and future perspectives. EMBO Mol. Med. 4, 1015–1028. https://doi.org/10.1002/emmm.201201379.

Diemer, C., Schneider, M., Seebach, J., Quaas, J., Frösner, G., Schätzl, H.M., Gilch, S., 2008. Cell type-specific cleavage of nucleocapsid protein by effector caspases during SARS coronavirus infection. J. Mol. Biol. 376, 23–34. https://doi.org/10.1016/j.jmb.2007.11.081.

Frumence, E., Viranaicken, W., Bos, S., Alvarez-Martinez, M.-T., Roche, M., Arnaud, J.-D., Gadea, G., Desprès, P., 2019. A chimeric Zika virus between viral strains MR766 and BeH819015 highlights a role for E-glycan loop in antibody-mediated virus neutralization. Vaccines 7. https://doi.org/10.3390/vaccines7020055.

Kim, D.W., Uetsuki, T., Kaziro, Y., Yamaguchi, N., Sugano, S., 1990. Use of the human elongation factor 1α promoter as a versatile and efficient expression system. Gene 91, 217–223. https://doi.org/10.1016/0378-1119(90)90091-5.

Lebeau, G., Vagner, D., Frumence, É., Ah-Pine, F., Guillot, X., Nobécourt, E., Raffray, L., Gasque, P., 2020. Deciphering SARS-CoV-2 Virologic and immunologic features. Int. J. Mol. Sci. 21. https://doi.org/10.3390/ijms21165932.

Leung, D.T.M., Tam, F.C.H., Ma, C.H., Chan, P.K.S., Cheung, J.L.K., Niu, H., Tam, J.S.L., Lim, P.L., 2004. Antibody response of patients with severe acute respiratory syndrome (SARS) targets the viral nucleocapsid. J. Infect. Dis. 190, 379–386. https://doi.org/10.1086/422040.

Long, Q.-X., Liu, B.-Z., Deng, H.-J., Wu, G.-C., Deng, K., Chen, Y.-K., Liao, P., Qiu, J.-F., Lin, Y., Cai, X.-F., Wang, D.-Q., Hu, Y., Ren, J.-H., Tang, N., Xu, Y.-Y., Yu, L.-H., Mo, Z., Gong, F., Zhang, X.-L., Tian, W.-G., Hu, L., Zhang, X.-X., Xiang, J.-L., Du, H.-X., Liu, H.-W., Lang, C.-H., Luo, X.-H., Wu, S.-B., Cui, X.-P., Zhou, Z., Zhu, M.-M., Wang, J., Xue, C.-J., Li, X.-F., Wang, L., Li, Z.-J., Wang, K., Niu, C.-C., Yang, Q.-J., Tang, X.-J., Zhang, Y., Liu, X.-M., Li, J.-J., Zhang, D.-C., Zhang, F., Liu, P., Yuan, J., Li, Q., Hu, J.-L., Chen, J., Huang, A.-L., 2020. Antibody responses to SARS-CoV-2 in patients with COVID-19. Nat. Med. 26, 845–848. https://doi.org/10.1038/s41591-020-0897-1.

Mark, J., Li, X., Cyr, T., Fournier, S., Jaentschke, B., Hefford, M.A., 2008. SARS coronavirus: unusual lability of the nucleocapsid protein. Biochem. Biophys. Res. Commun. 377, 429–433. https://doi.org/10.1016/j.bbrc.2008.09.153.

Rogers, T.F., Zhao, F., Huang, D., Beutler, N., Burns, A., He, W., Limbo, O., Smith, C., Song, G., Woehl, J., Yang, L., Abbott, R.K., Callaghan, S., Garcia, E., Hurtado, J., Parren, M., Peng, L., Ramirez, S., Ricketts, J., Ricciardi, M.J., Rawlings, S.A., Wu, N.C., Yuan, M., Smith, D.M., Nemazee, D., Teijaro, J.R., Voss, J.E., Wilson, I.A., Andrabi, R., Briney, B., Landais, E., Sok, D., Jardine, J.G., Burton, D.R., 2020. Isolation of potent SARS-CoV-2 neutralizing antibodies and protection from disease in a small animal model. Science 369, 956–963. https://doi.org/10.1126/science.abc7520.

Surjit, M., Kumar, R., Mishra, R.N., Reddy, M.K., Chow, V.T.K., Lal, S.K., 2005. The severe acute respiratory syndrome coronavirus nucleocapsid protein is phosphorylated and localizes in the cytoplasm by 14-3-3-mediated translocation. J. Virol. 79, 11476–11486. https://doi.org/10.1128/JVI.79.17.11476-11486.2005.

Walls, A.C., Park, Y.-J., Tortorici, M.A., Wall, A., McGuire, A.T., Veesler, D., 2020. Structure, function, and antigenicity of the SARS-CoV-2 spike glycoprotein. Cell 181. https://doi.org/10.1016/j.cell.2020.02.058, 281-292.e6.

Wang, C., Wang, Z., Wang, G., Lau, J.Y.-N., Zhang, K., Li, W., 2021. COVID-19 in early 2021: current status and looking forward. Sign. Transduct. Target. Ther. 6, 1–14. https://doi.org/10.1038/s41392-021-00527-1.

Wurm, F.M., 2004. Production of recombinant protein therapeutics in cultivated mammalian cells. Nat. Biotechnol. 22, 1393–1398. https://doi.org/10.1038/nbt1026.

Zhao, B., Zhang, X., Krummenacher, C., Song, S., Gao, L., Zhang, H., Xu, M., Feng, L., Feng, Q., Zeng, M., Xu, Y., Zeng, Y., 2018. Immunization with fc-based recombinant Epstein–Barr virus gp350 elicits potent neutralizing humoral immune response in a BALB/c mice model. Front. Immunol. 9 https://doi.org/10.3389/fimmu.2018.00932.

Zhou, P., Yang, X.-L., Wang, X.-G., Hu, B., Zhang, L., Zhang, W., Si, H.-R., Zhu, Y., Li, B., Huang, C.-L., Chen, H.-D., Chen, J., Luo, Y., Guo, H., Jiang, R.-D., Liu, M.-Q., Chen, Y., Shen, X.-R., Wang, X., Zheng, X.-S., Zhao, K., Chen, Q.-J., Deng, F., Liu, L.-L., Yan, B., Zhan, F.-X., Wang, Y.-Y., Xiao, G.-F., Shi, Z.-L., 2020. A pneumonia outbreak associated with a new coronavirus of probable bat origin. Nature 579, 270–273. https://doi.org/10.1038/s41586-020-2012-7.